



Research Article

Antidepressant-like effect of ginsenoside Rb1 on potentiating synaptic plasticity via the miR-134–mediated BDNF signaling pathway in a mouse model of chronic stress-induced depression

Guoli Wang^{a,1}, Tianyue An^{a,1}, Cong Lei^a, Xiaofeng Zhu^{b,c}, Li Yang^a, Lianxue Zhang^{d,*}, Ronghua Zhang^{a,**}

^a College of Pharmacy, Jinan University, Guangzhou, China

^b College of Traditional Chinese Medicine, Jinan University, Guangzhou, China

^c Department of the First Affiliated Hospital, Jinan University, Guangzhou, China

^d College of Chinese Medicinal Materials, Jilin Agricultural University, Changchun, China



ARTICLE INFO

Article history:

Received 12 November 2020

Received in revised form

6 March 2021

Accepted 14 March 2021

Available online 20 March 2021

Keywords:

Ginsenoside Rb1

Depression

miR-134

BDNF–TrkB signaling

Synaptic plasticity

ABSTRACT

Background: Brain-derived neurotrophic factor (BDNF)–tropomyosin-related kinase B (TrkB) plays a critical role in the pathogenesis of depression by modulating synaptic structural remodeling and functional transmission. Previously, we have demonstrated that the ginsenoside Rb1 (Rb1) presents a novel antidepressant-like effect via BDNF–TrkB signaling in the hippocampus of chronic unpredictable mild stress (CUMS)-exposed mice. However, the underlying mechanism through which Rb1 counteracts stress-induced aberrant hippocampal synaptic plasticity via BDNF–TrkB signaling remains elusive.

Methods: We focused on hippocampal microRNAs (miRNAs) that could directly bind to BDNF and are regulated by Rb1 to explore the possible synaptic plasticity-dependent mechanism of Rb1, which affords protection against CUMS-induced depression-like effects.

Results: Herein, we observed that brain-specific miRNA-134 (miR-134) could directly bind to BDNF 3'UTR and was markedly downregulated by Rb1 in the hippocampus of CUMS-exposed mice. Furthermore, the hippocampus-targeted miR-134 overexpression substantially blocked the antidepressant-like effects of Rb1 during behavioral tests, attenuating the effects on neuronal nuclei-immunoreactive neurons, the density of dendritic spines, synaptic ultrastructure, long-term potentiation, and expression of synapse-associated proteins and BDNF–TrkB signaling proteins in the hippocampus of CUMS-exposed mice.

Conclusion: These data provide strong evidence that Rb1 rescued CUMS-induced depression-like effects by modulating hippocampal synaptic plasticity via the miR-134-mediated BDNF signaling pathway.

© 2021 The Korean Society of Ginseng. Publishing services by Elsevier B.V. This is an open access article under the CC BY-NC-ND license (<http://creativecommons.org/licenses/by-nc-nd/4.0/>).

Abbreviations: AAV9, adeno-associated viral serotype 9; AKT, protein kinase B; AMPAR, α -amino-3-hydroxy-5-methyl-4-isoxazole propionic acid receptor; ANOVA, analysis of variance; BDNF, brain-derived neurotrophic factor; CaMKII, Ca²⁺/calmodulin-dependent protein kinase II; CMC-Na, carboxymethyl cellulose sodium; CREB, cAMP response element-binding protein; CUMS, chronic unpredictable mild stress; DG, dentate gyrus; ERK1/2, extracellular regulatory protein kinase; fEPSPs, field excitatory postsynaptic potentials; FST, forced swimming test; GAP-43, growth-associated protein 43; GluR1, AMPAR subunit glutamate receptor 1; GSK-3 β , glycogen synthase kinase-3 β ; HFS, high-frequency stimulation; IACUC, Institutional Animal Care and Use Committee; ICR, Institute of Cancer Research; i.g., intragastrically; LIMK1, LIM-kinase 1; LTD, long-term depression; LTP, long-term potentiation; MAP-2, microtubule-associated protein-2; MAPK, mitogen-activated protein kinase; MDD, major depressive disorder; miRNAs, microRNAs; miR-134, miRNA-134; NeuN, neuronal nuclei; NMDAR, N-methyl-D-aspartic acid receptor; NR2A, NMDAR subunit 2A; NR2B, NMDAR subunit 2B; OFT, open field test; PI3K, phosphatidylinositol 3-kinase; PSD, postsynaptic density; PSD-95, postsynaptic density protein 95; qRT-PCR, quantitative real-time PCR; Rb1, ginsenoside Rb1; SEM, standard error of the mean; SPT, sucrose preference test; Syn, synaptophysin; TrkB, tropomyosin-related kinase B; TST, tail suspension test.

* Corresponding author. College of Chinese Medicinal Materials, Jilin Agricultural University, Changchun, 130118, China.

** Corresponding author. College of Pharmacy, Jinan University, Guangzhou, 510632, China.

E-mail addresses: zlxbooksea@163.com (L. Zhang), tzrh@jnu.edu.cn (R. Zhang).

¹ These authors contributed equally to this work.

<https://doi.org/10.1016/j.jgr.2021.03.005>

1226-8453/© 2021 The Korean Society of Ginseng. Publishing services by Elsevier B.V. This is an open access article under the CC BY-NC-ND license (<http://creativecommons.org/licenses/by-nc-nd/4.0/>).

1. Introduction

Major depressive disorder is a complex and heterogeneous disease. Neurobiological studies have observed that the pathogenesis of depression mainly involves alterations in the signaling system, neuroplasticity, neuroinflammation, and the neuroendocrine system [1–3]. Notably, the cellular mechanisms underlying these alterations may be strongly associated with changes in neuroplasticity [4]. Novel findings have revealed that neuroplasticity, which is the ability of adult synapses to adapt to external stimuli dynamically, is dysregulated during depression and restored by antidepressants [5].

Synaptic plasticity is controlled by complex regulation of diverse signaling pathways, and disruptions of some major pathways can enhance vulnerability to depression, including the loss of neurotrophic factors. Brain-derived neurotrophic factor (BDNF), a key determinant of neuroplasticity, is highly expressed in the hippocampus. BDNF is secreted locally, at and near active synapses, and regulates neuronal survival and differentiation, with functions in the activity-dependent plasticity processes [6,7]. A recent study has shown that BDNF could serve as a transducer to link antidepressants and neuroplastic changes [8]. Tropomyosin-related kinase B (TrkB), a functional receptor of BDNF, is widely distributed on presynaptic and postsynaptic membranes and activated by BDNF [9]. Evidence has confirmed that BDNF–TrkB signaling participates in regulating synaptic structural remodeling and functional transmission by activating at least two intracellular signaling pathways, namely, the mitogen-activated protein kinase (MAPK)/extracellular signal-regulated protein kinase (ERK) and phosphatidylinositol 3-kinase (PI3K)/protein kinase B (PKB/AKT) pathways [10–12]. Both pathways are associated with numerous downstream targets affecting neuronal function. For example, activation of the downstream transcription factor cAMP response element-binding protein (CREB) contributes to the maintenance of activity-dependent synaptic plasticity and transcription of synapse-related protein-encoding genes, including *BDNF* [13]. Multiple BDNF functions are involved in promoting synaptic efficacy, primarily by inducing postsynaptic potentiation to promote long-term potentiation (LTP) [14]; enhancing the conductance of N-methyl-D-aspartic acid receptors (NMDARs) [15] and translation of α -amino-3-hydroxy-5-methyl-4-isoxazole propionic acid receptors (AMPA receptors) to increase postsynaptic responses [16]; and favoring synaptic remodeling of the ultrastructure to promote synaptogenesis [17]. Therefore, the beneficial effects of the BDNF–TrkB signaling pathway on the attenuation of depression-induced dysfunctions are expected to prevent depression-induced impairment of hippocampal synaptic plasticity; this could be developed as a potential therapeutic strategy for antidepressants.

Ginsenoside Rb1 (Rb1), the primary bioactive ingredient in *Panax ginseng* Meyer, reportedly elicits an antidepressant-like effect by regulating hippocampal monoamine and amino acid neurotransmitter levels in chronic unpredictable mild stress (CUMS)-exposed mice in our previous study [18,19]. In addition, our studies on CUMS-exposed mice demonstrated that the antidepressant-like effect of Rb1 is related to BDNF–TrkB signaling in the hippocampus [20]. However, the underlying mechanism through which Rb1 counteracts stress-induced aberrant hippocampal synaptic plasticity via the BDNF–TrkB signaling pathway remains elusive. MicroRNAs (miRNAs) are small, highly conserved noncoding RNAs of ~20 nucleotides, regulating gene expression by repressing the translation of target mRNAs into protein or degrading target mRNAs. It has been confirmed that miRNAs play an important role in the pathophysiology of stress-related disorders, owing to their ability to regulate multiple pathways associated with synaptic plasticity [21,22]. In the present study, we focused on hippocampal

miRNAs that could directly bind to *BDNF* and are regulated by Rb1, to explore the possible synaptic plasticity-dependent Rb1 mechanism affording protection against CUMS-induced depression-like effects.

2. Materials and methods

2.1. Animals

Male adult Institute of Cancer Research (ICR) mice, weighing 20 ± 2 g (5-week-old), were purchased from SJA Laboratory Animal Co., Ltd. (Hunan, China). Animals were housed in clear polycarbonate cages ($22.5 \times 33.8 \times 14.0$ cm in size) in groups of 8 individuals, under a controlled 12-hour light/dark cycle (light from 7:00 am to 7:00 pm), at $55 \pm 10\%$ relative humidity and $25 \pm 2^\circ\text{C}$ room temperature. All experimental protocols and animal treatments were performed according to the Experimental Animal Application Criteria and Institutional Animal Care and Use Committee (IACUC) of Jinan University (Permit No. 2019624).

2.2. Procedure for CUMS exposure

The CUMS procedure was adapted from a previous report [23]. Briefly, mice were exposed to 10 series of mild and unpredictable stressors, including food or water deprivation for 12 h, a soiled cage for 24 h, plantar electrical stimulation for 10 min, swimming in cold water (4°C) for 5 min, overnight illumination for 36 h, nipping of the tail for 2 min, cage tilt (45°) for 12 h, white noise for 12 h; and LED stroboscopic stimulation for 2 h. The mice received two or three random stressors daily to ensure unpredictability.

2.3. Dual-luciferase reporter gene assay

The predicted targets of mmu-miR-134 (miR-134) were analyzed by RNAhybrid 2.2 (https://bibiserv.cebitec.uni-bielefeld.de/applications/rnahybrid/pages/rnahybrid_function_rnahybrid_result.jsf). The sequences of wild-type (BDNF-3'UTR-WT) or mutated (BDNF-3'UTR-Mut) *BDNF* 3'UTR were constructed to pmirGLO vector (Promega, Madison, WI, USA). The luciferase assay was performed with 293 T cells using the Dual-Luciferase Reporter 2000 Assay System (Promega, Madison, WI, USA). All experiments were performed in duplicate, with data pooled from three independent experiments.

2.4. Stereotactic injection

The adeno-associated viral serotype 9 (AAV9) vectors, including AAV-miR-134-down (miR-134 knockdown), AAV-miR-134-up (miR-134 overexpress), and AAV-vehicle, were constructed by Genechem Co., Ltd. (Shanghai, China). Viral injections were performed as described in previous reports [24]. AAV viruses (10^{12} vector genome (vg)/mL, $1.0 \mu\text{L}$ of AAV per hippocampus) were bilaterally infused into the hippocampus (Bregma: 2.3 mm; Medial/Lateral: ± 1.8 mm; Dorsal/Ventral: 2.0 mm) (Fig. 1A and B). Following the induction of CUMS, the injection site was determined by detecting red fluorescent protein (mCherry) expression using a laser confocal microscope.

2.5. Drugs and treatment

In the present study, Rb1 ($\text{C}_{54}\text{H}_{92}\text{O}_{23}$, molecular weight 1109.31, Fig. 1C) was derived from the same batch prepared in our previous study [20] and was dissolved in 0.5% carboxymethyl cellulose sodium (CMC-Na) at a concentration of 0.9 mM. After one week of CUMS exposure, mice were divided into eight groups ($n=16$ per

group): Control group, CUMS–vehicle group, Rb1-treated group, AAV–vehicle group, AAV–miR-134-down group, AAV–miR-134-up group, Rb1+AAV–miR-134-down group, and Rb1+AAV–miR-134-up group. Rb1 was intragastrically (i.g.) administered to CUMS-exposed mice once a day at 9:00–11:00 am, from day 7 to day 42. After 60 min of administering Rb1 on day 7, the AAV-treated group underwent a one-time stereotactic injection of the AAV virus (Fig. 1D). Behavioral experiments were conducted 60 min after the last administration with Rb1 or CMC-Na.

2.6. Behavioral assays

All behavioral tests were conducted in a separate room, and behavioral equipment was connected to a digital camera monitoring system. On the last day of CUMS exposure, mice were subjected to the open field test (OFT), tail suspension test (TST), forced swimming test (FST), and sucrose preference test (SPT) to evaluate depression-like behaviors [20].

2.7. Immunohistochemistry

Immunohistochemical staining for anti-neuronal nuclei (NeuN) and quantitative analysis of immunohistochemical data were performed as previously reported [25]. NeuN-immunoreactive neurons were scanned and counted in a $100 \times 100 \mu\text{m}^2$ area of the hippocampal CA1, CA3, and dentate gyrus (DG) using the

CaseViewer 2.3.0 image analysis system (3DHISTECH, Budapest, Hungary).

2.8. Golgi staining

Golgi staining was performed using the FD Rapid GolgiStain™ Kit (FD Neuro Technologies, Columbia, MD, USA). Images of dendrites within CA1, CA3, and DG regions were captured using the CaseViewer 2.3.0 system (3DHISTECH, Budapest, Hungary), and the number of spines on multiple dendritic branches were quantified using ImageJ (NIH, Bethesda, MD, USA).

2.9. Electron microscopy

The hippocampal tissues for electron microscopy were prepared as described in a previous report [26]. The ultrastructure of hippocampal neurons was observed under a transmission electron microscope (HITACHI HT7700, TEM, Japan). Ultrastructure parameters of the synapse, including postsynaptic density (PSD) length and thickness and the synaptic cleft width in hippocampal CA1 and CA3 regions, were examined using Image-pro plus 6.0 (Media Cybernetics, Inc., Rockville, MD, USA).

2.10. Electrophysiology

Hippocampal slices were prepared from mice aged 12–13 weeks, as described by Egawa et al. [27]. Extracellular field

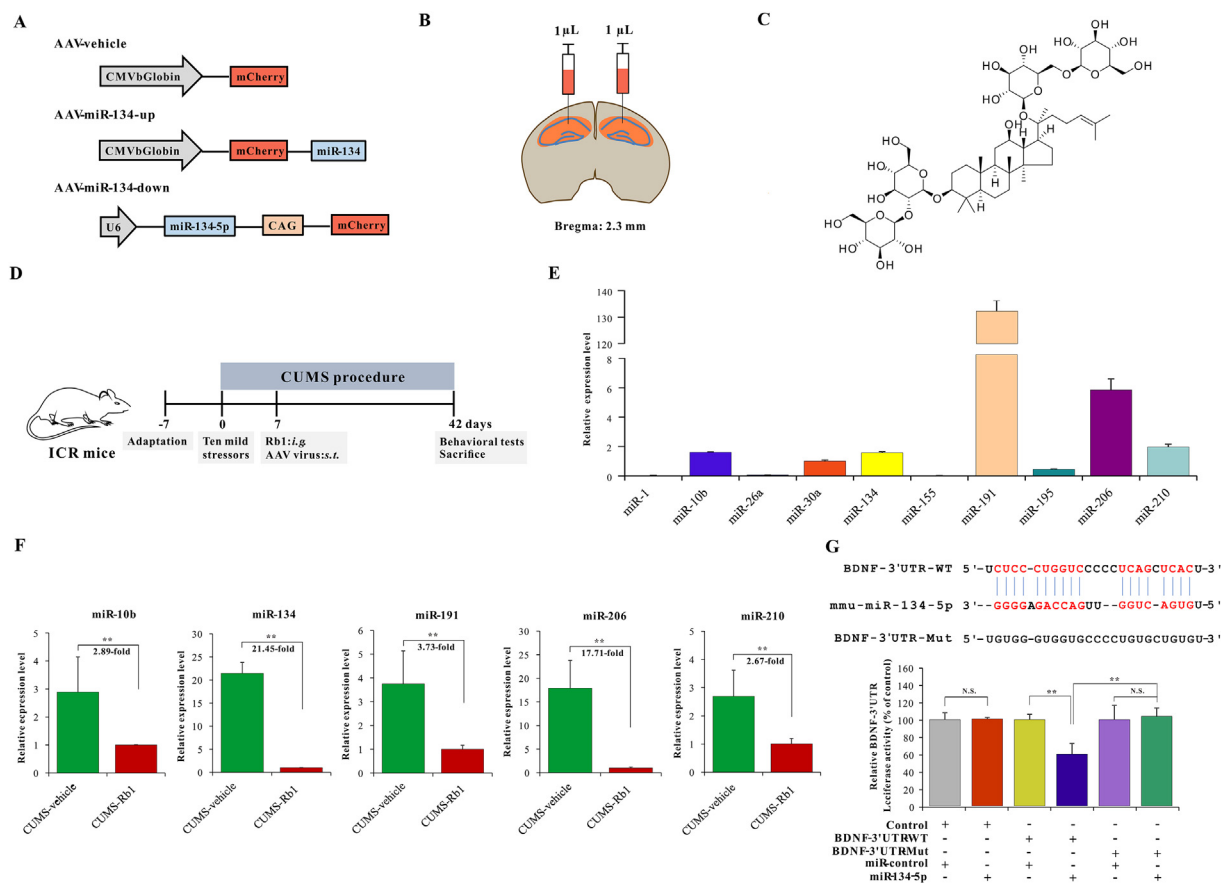


Fig. 1. mmu-miR-134 directly targeted *BDNF* 3'UTR. (A) The AAV vector of recombinant miR-134. (B) Schematic diagram of stereotactic injection of AAV into the hippocampus. (C) The molecular structure of Rb1. (D) Experimental schedule. (E) mRNA expression of miRNAs targeting *BDNF* 3'UTR in the hippocampus of normal mice. (F) Rb1 inhibited the expression of mmu-miR-134-5p in the hippocampus of CUMS-exposed mice. (G) Luciferase activity of reporter gene with *BDNF*-3'UTR-WT or *BDNF*-3'UTR-Mut and mmu-miR-134. Data are presented as means \pm SEM ($n=3-5$). * $p < 0.05$ and ** $p < 0.01$ were considered statistically significant.

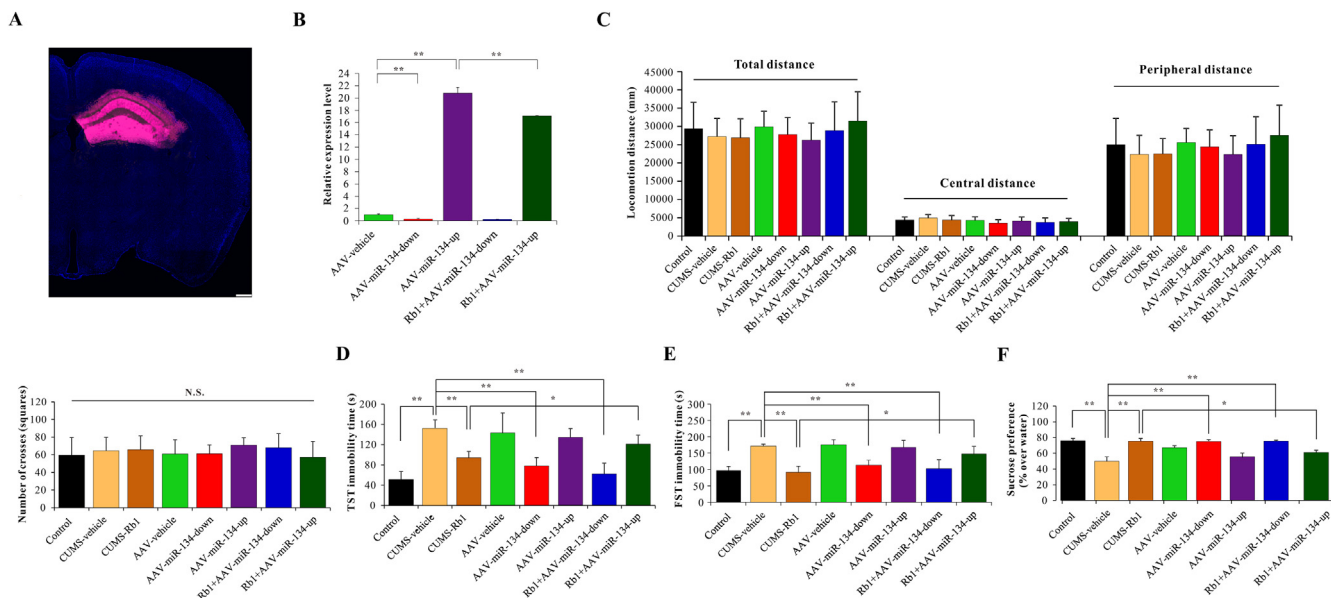


Fig. 2. Antidepressant-like effects of Rb1 on behavioral tests in CUMS-exposed mice were suppressed by miR-134 overexpression. (A) Schematic diagram of localization and expression of AAV-miR-134 in the mouse hippocampus (scale bar = 200 μ m). (B) mRNA expression of AAV-miR-134 in different treatment groups. Behavioral tests including (C) OFT, (D) TST, (E) FST, and (F) SPT. Data are presented as means \pm SEM ($n=7-9$). * $p < 0.05$ and ** $p < 0.01$ were considered statistically significant.

excitatory postsynaptic potentials (fEPSPs) at CA3–CA1 synaptic responses were recorded using a Multiclamp 700B amplifier (Molecular Devices, Sunnyvale, CA, USA). The measurement was performed within 30 min, at a stimulus frequency of 0.033 Hz and a stimulation interval of 20 s between trains. After stabilizing responses, LTP was induced by high-frequency stimulation (HFS, 100 Hz with 100 pulses) with a 20 s interval between trains, and the slope of fEPSP was recorded by test stimulation for a further 60 min. The field potential data were analyzed using the software pClamp 9.2 (Molecular Devices, Sunnyvale, CA, USA). The ratio of the average fEPSP slope of the last 30 min after HFS to the average fEPSP slope of 30 min of the initial baseline was calculated.

2.11. Quantitative real-time PCR (qRT-PCR) and western blot analysis

Total RNA was extracted from the hippocampus using TRIzol reagent (Life Technologies, Carlsbad, CA, USA), and 1 μ g of total RNA was used to generate cDNA by reverse transcription with the miRNA First Strand cDNA Synthesis (Tailing Reaction) Kit (Sangon Biotech Co., Ltd., Shanghai, China). Experiments were performed on an Applied Biosystems 7500 real-time PCR system (Life Technologies, Carlsbad, CA, USA) with specific miRNA primers (Table S1).

Total levels of hippocampal synapse-related proteins and BDNF–TrkB signaling proteins were determined by western blotting as previously described [20]. Specific information regarding primary antibodies is listed in Table S2. Images were captured with a ChemiDocTM MP imaging system (Bio-Rad, Hercules, CA, USA), and immunoreactive bands were quantified by ImageJ (NIH, Maryland, USA). β -actin was selected as the internal control.

2.12. Statistical analysis

All statistical procedures were performed using GraphPad Prism 7.0 (GraphPad Software, San Diego, CA, USA). All values are expressed as mean \pm standard error of the mean (SEM). Statistical comparison between groups was evaluated using one-way or two-

way analysis of variance (ANOVA) with Dunnett's or Bonferroni's post hoc test. A p -value < 0.05 was considered statistically significant.

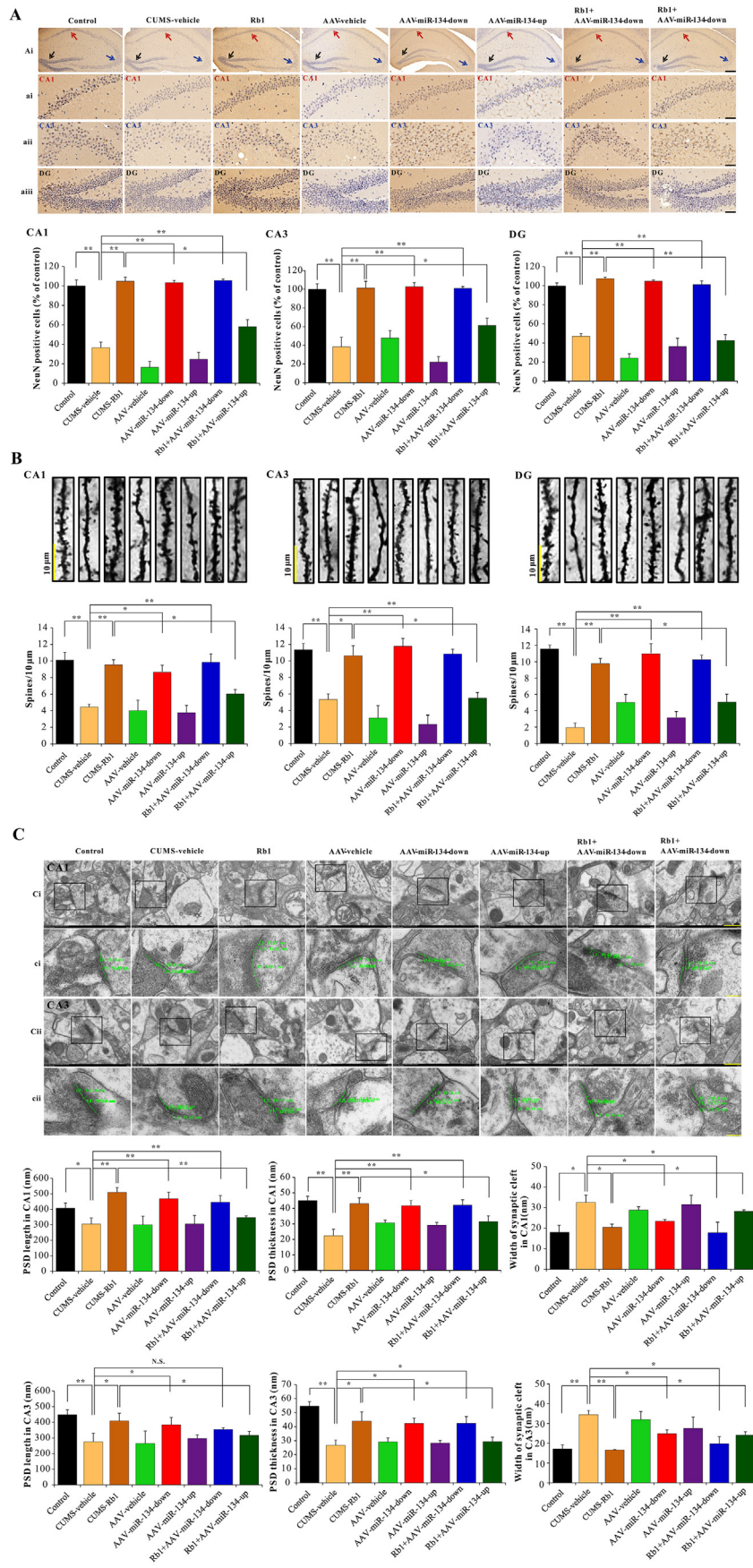
3. Results

3.1. mmu-miR-134 directly targeted BDNF 3'UTR

To explore the molecular mechanism of Rb1 in regulating hippocampal synaptic plasticity in depression through BDNF, we focused on miRNAs that directly bind to BDNF and are regulated by Rb1 in the hippocampus of CUMS-exposed mice.

Evidence has demonstrated that hsa-miR-1, hsa-miR-10b, hsa-miR-26a, hsa-miR-134, hsa-miR-155, hsa-miR-191, hsa-miR-195, hsa-miR-206, hsa-miR-210, and mmu-miR-30a can directly target BDNF 3'UTR and regulate its expression [28–32]. In the present study, gene expression analysis revealed that homologous miRNAs of hsa-miR-10b, hsa-miR-134, hsa-miR-191, hsa-miR-206, and hsa-miR-210 were highly expressed in the mouse hippocampus (Fig. 1E). The mouse model of CUMS-induced depression was established to further detect the expression pattern of these miRNAs in the mouse hippocampus. Our results revealed that transcripts of mmu-miR-10b, mmu-miR-134, mmu-miR-191, mmu-miR-206, and mmu-miR-210 were markedly inhibited by Rb1, and the most significant inhibitory effect was exerted on mmu-miR-134 (Fig. 1F). Therefore, we selected mmu-miR-134 as a candidate for the following functional verification.

BDNF was identified as a potential target of mmu-miR-134 by RNAhybrid 2.2 (Fig. 1G). Luciferase reporter assay was employed to determine whether miR-134 can directly bind to BDNF 3'UTR using the BDNF-3'UTR-WT or BDNF-3'UTR-Mut and mmu-miR-134. As shown in Fig. 1G, compared with the miR-control group, the luciferase activity of BDNF-3'UTR-WT and miR-134-5p was significantly decreased, indicating that miR-134 interacted with BDNF. As the luciferase activity of BDNF-3'UTR-Mut and miR-134 recovered to that of the miR-control group, the mutated site in BDNF 3'UTR was deemed the binding site of miR-134-5p.



3.2. Antidepressant-like effects of Rb1 on behavioral tests in CUMS-exposed mice were suppressed by miR-134 overexpression

Next, to explore the role of miR-134/BDNF signaling pathway in the antidepressant-like effects of Rb1, the recombinant AAV-miR-134 was infused bilaterally into the mouse hippocampus on day 7 of CUMS procedure. As displayed in Fig. 2A, AAV-miR-134 was expressed in the hippocampus on day 21 of post-infusion under CUMS exposure. Compared with the AAV-vehicle group, the hippocampal miR-134 mRNA level in the AAV-miR-134-down-treated group was suppressed, while that in the AAV-miR-134-up-treated group was markedly enhanced. Moreover, Rb1 reduced the increased miR-134 mRNA level in the AAV-miR-134-up-treated group, indicating that Rb1 could negatively regulate the expression of miR-134 in CUMS-exposed mice (Fig. 2B).

To further investigate the role of miR-134 in the antidepressant-like effects of Rb1 in CUMS-induced depression-like behaviors, OFT, TST, FST, and SPT were performed at the end of the CUMS protocol. The OFT was performed prior to the FST or TST to exclude sedative or motor abnormalities. As shown in Fig. 2C, there were no differences in the locomotor distance of central and peripheral areas or the number of squares crossed between CMC-Na-, Rb1-, and miR-134-treated groups. The CUMS-treated group displayed a significant increase in the immobility time of TST (Fig. 2D) and FST (Fig. 2E), with decreased sucrose consumption observed in the SPT (Fig. 2F); Rb1 treatment significantly reversed these depression-like behaviors. Moreover, miR-134 deficiency or combination with Rb1 positively impacted the TST, FST, and SPT parameters assessed. Surprisingly, the antidepressant-like effects of Rb1 in the TST, FST, and SPT were suppressed by miR-134 overexpression in CUMS-exposed mice.

3.3. Antidepressant-like effects of Rb1 on synaptic structural changes in the hippocampal neurons of CUMS-exposed mice were attenuated by miR-134 overexpression

Immunohistochemical analysis of NeuN, a neuron-specific nuclear protein, in the hippocampus was compared between CUMS-exposed and control groups. On day 42, compared with the control group, the CUMS-exposed group showed a significant decrease in NeuN-immunoreactive neurons in the stratum pyramidale of CA1 and CA3 regions, particularly in the granule cell layer of the DG subfield, and subchronic treatment with Rb1 abolished these deficits. In addition, miR-134 deficiency revealed a marked neuroprotective effect in these regions. As expected, the neuroprotective effect of Rb1 in the CA1, CA3, and DG regions of CUMS-exposed mice was dramatically suppressed by miR-134 overexpression (Fig. 3A).

In line with histological changes in NeuN-immunoreactive neurons, we explored changes in dendritic spine density in hippocampal neurons between CUMS-exposed and control groups, using Golgi staining. As shown in Fig. 3B, the dendritic spine densities in the CA1, CA3, and DG regions were significantly reduced in CUMS-exposed mice; subchronic treatment with Rb1 considerably reduced the above deficits. Furthermore, miR-134 deficiency revealed results similar to the Rb1-treated mice under CUMS exposure. However, the positive effect of Rb1 on the dendritic spine density of CUMS-exposed mice was substantially reduced by miR-134 overexpression.

Next, electron microscopy was performed to assess the ultrastructural indicators of synaptic plasticity in the hippocampus (Fig. 3C). Based on synaptic ultrastructure images, differences in the hippocampal stratum pyramidale of CA1 and CA3 regions were observed between different groups. Morphometric analysis revealed that Rb1 significantly alleviated the decreased PSD length and increased width of the synaptic cleft in the CA1 and CA3 regions of CUMS-exposed mice. As expected, miR-134 deficiency demonstrated similar results to the Rb1-treated CUMS-exposed mice. Moreover, the positive effect of Rb1 on the synaptic ultrastructure in the depressed mice was substantially inhibited following miR-134 overexpression.

3.4. Antidepressant-like effects of Rb1 on synaptic functional changes in the hippocampal neurons of CUMS-exposed mice were antagonized by miR-134 overexpression

Electrophysiological recordings of LTP induction in the CA1 region were examined by measuring fEPSP after CA3 Schaffer collateral stimulation to assess the effects of miR-134 on synaptic properties and synaptic transmission efficiency (functional changes) in hippocampal neurons (Fig. 4A). The Schaffer collateral-CA1 synaptic property was analyzed by plotting fractional changes in the fEPSP slopes against stimulating intensities in hippocampal slices from controls or CUMS-exposed mice. We observed that Rb1 markedly restored the reduced fEPSP slope induced by CUMS. miR-134 deficiency demonstrated results similar to Rb1-treated CUMS-exposed mice. As expected, the enhancement of hippocampal LTP in the CA1 neurons in Rb1-treated CUMS-exposed mice was further antagonized by miR-134 overexpression (Fig. 4B and C).

To further determine the role of miR-134 in hippocampal synaptic plasticity regulated by Rb1, the expression of hippocampal synapse-associated proteins was analyzed on the last day of the behavioral tests. For all groups, no significant differences in the expression of synaptophysin (Syn) were observed (Fig. 4D). However, the hippocampal expression of synapse-associated proteins, including postsynaptic density protein-95 (PSD-95), growth-associated protein-43 (GAP-43), microtubule-associated protein-2 (MAP-2), NMDAR subunit 2A (NR2A), NMDAR subunit 2B (NR2B), AMPAR subunit glutamate receptor 1 (GluR1), and Ca²⁺/calmodulin-dependent protein kinase II (CaMKII), was substantially decreased in CUMS-exposed mice compared with that in the controls; subchronic treatment with Rb1 markedly upregulated these proteins. Consistent with these results, the low expression of miR-134 presented a similar effect in Rb1-treated CUMS-exposed mice. Conversely, the positive effects of Rb1 on synapse-related proteins in the hippocampus of depression-induced mice were inhibited by miR-134 overexpression (Fig. 4E–K).

3.5. miR-134-mediated BDNF signaling was involved in the antidepressant-like effects of Rb1 in CUMS-exposed mice

As miR-134-5p could directly bind to BDNF 3'UTR, we next assessed whether Rb1 produced antidepressant-like effects through the miR-134-mediated BDNF signaling pathway. As shown in Fig. 5A–G, BDNF signaling was analyzed in the hippocampus of control or CUMS-exposed mice. Our findings revealed that expression levels of BDNF and its downstream proteins,

Fig. 3. Antidepressant-like effects of Rb1 on synaptic structural changes in the hippocampal neurons of CUMS-exposed mice were attenuated by miR-134 overexpression. (A) NeuN immunohistochemistry in the hippocampal CA1, CA3, and DG regions (Ai: scale bar = 200 μ m; ai–aiii: scale bar = 50 μ m). (B) Representative Golgi staining images of dendritic spines in the hippocampal CA1, CA3, and DG regions (scale bar = 10 μ m). (C) Representative electron microscopic images of PSD length, PSD thickness, and the width of the synaptic cleft in the hippocampal CA1 and CA3 regions (Ci and Cii: scale bar = 200 μ m; ci and cii: scale bar = 50 μ m). Data are presented as means \pm SEM ($n=6$). * $p < 0.05$ and *** $p < 0.01$ were considered statistically significant.

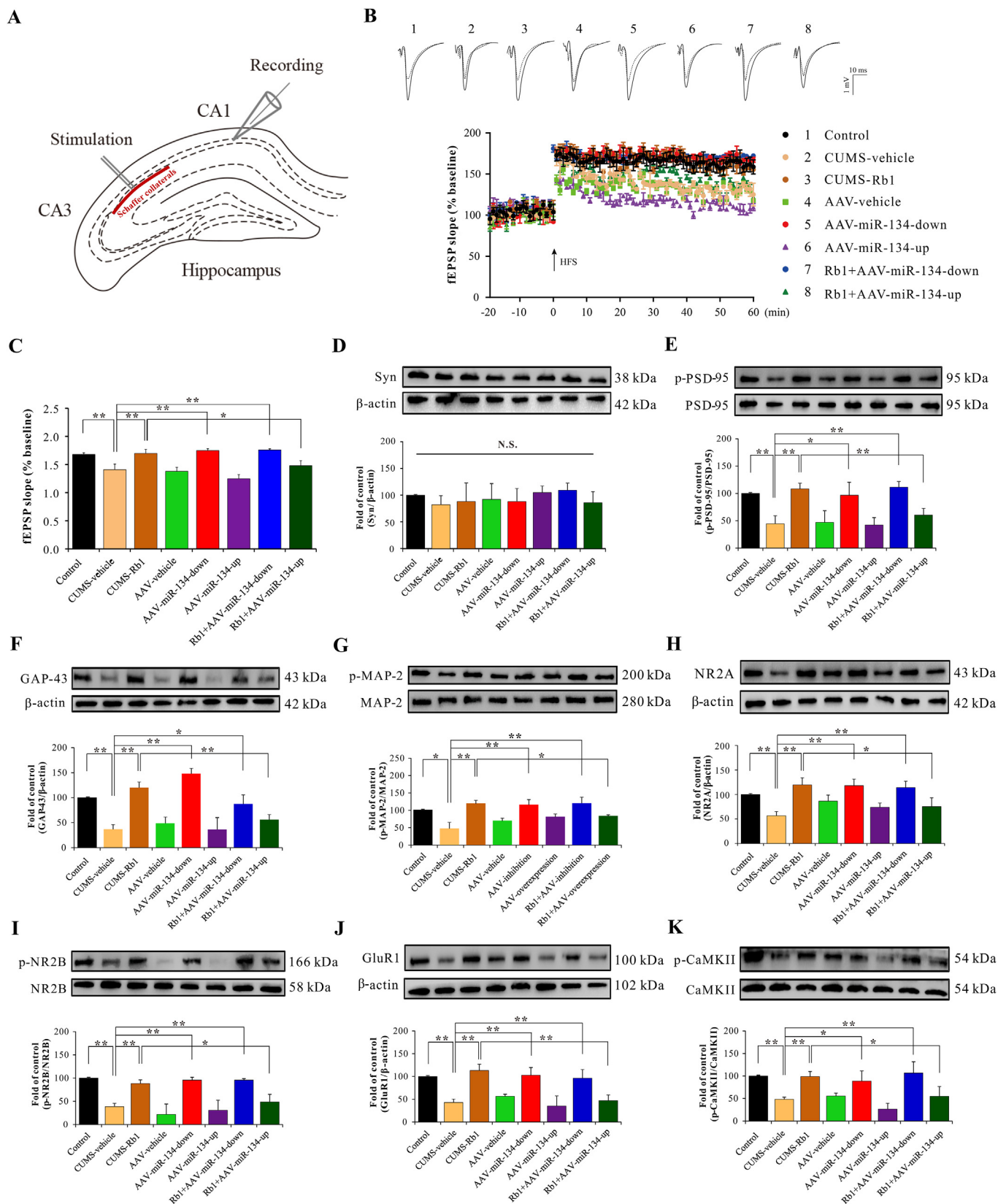


Fig. 4. Antidepressant-like effects of Rb1 on synaptic functional changes in the hippocampal neurons of CUMS-exposed mice were attenuated by miR-134 overexpression. (A) Schematic diagram of LTP induction in the hippocampal Schaffer collateral–CA1 synaptic pathway. (B) The trend of fEPSP waveform and slope in the hippocampal CA1 region. (C) Recording of the fEPSP slope in the hippocampal CA1 region. Expression of synapse-associated proteins, including (D) Syn, (E) PSD-95, (F) GAP-43, (G) MAP-2, (H) NR2A, (I) NR2B, (J) GluR1, and (K) CaMKII. Data are presented as means ± SEM (n=3–5); *p < 0.05 and **p < 0.01 were considered statistically significant.

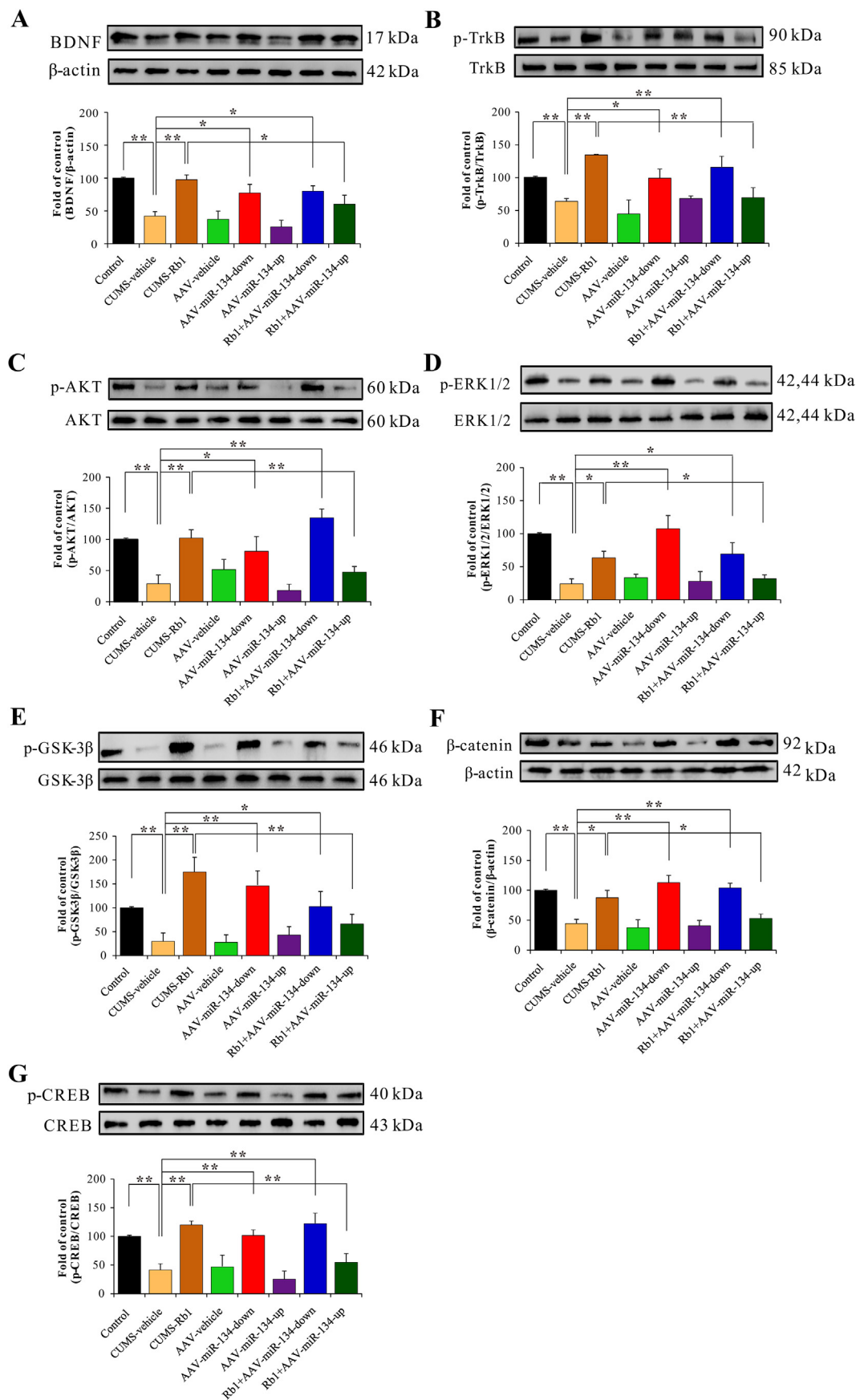


Fig. 5. miR-134-mediated BDNF signaling was involved in the antidepressant-like effects of Rb1 in CUMS-exposed mice. Expression of proteins, including (A) BDNF, (B) TrkB, (C) AKT, (D) ERK1/2, (E) GSK-3 β , (F) β -catenin, and (G) CREB. Data are presented as means \pm SEM ($n=3-5$). * $p < 0.05$ and ** $p < 0.01$ were considered statistically significant.

including TrkB, AKT, ERK1/2, glycogen synthase kinase-3β (GSK-3β), β-catenin, and CREB, were markedly upregulated in CUMS-exposed Rb1-treated mice. Furthermore, miR-134 deficiency demonstrated a positive effect on the regulation of BDNF signaling. In contrast, the effect of Rb1 on the regulation of hippocampal BDNF signaling was comprehensively antagonized by miR-134 overexpression. These data demonstrated that BDNF was the direct downstream target of miR-134 and was negatively modulated by miR-134. These results further revealed that miR-134-mediated BDNF signaling might be involved in the antidepressant-like effects of Rb1 in CUMS-exposed mice.

4. Discussion

Recent clinical and animal studies have revealed that pyramidal neurons could be negatively influenced by chronic stress, resulting in shrinkage of dendritic cells and fewer spines [33,34]. Structural plasticity is not only related to the modifiability and variability of synapses in terms of morphology, quantity, interface structure, and axon-dendritic connection functions but also to changes in synaptic ultrastructure. Moreover, structural plasticity allows the continuous modification of connections and neural circuits between nerves to increase the adaptability of synapses to the environment [35]. A recent study has revealed that CUMS worsens synaptic strength and neurotransmission efficiency in the neural circuit by

altering the synaptic ultrastructure, decreasing PSD length and thickness, and increasing the width of the synaptic cleft in the rat hippocampus [26]. These findings support the notion that the integrity of the synaptic structure is the basis for determining the efficiency of synaptic transmission [36]. Consistent with these reports, our *in vitro* results revealed that Rb1 not only increased dendritic spine density in the hippocampal CA1, CA3, and DG regions but additionally enhanced the length and thickness of PSD and decreased the width of the synaptic cleft in the hippocampal CA1 and CA3 regions of CUMS-exposed mice. Furthermore, miR-134 deficiency produced a similar effect on the synaptic ultrastructure of Rb1-treated CUMS-exposed mice. Interestingly, Rb1 could negatively regulate the expression of miR-134 and the positive effect of Rb1 on the synaptic structure was strongly reversed following miR-134 overexpression in CUMS-exposed mice; this indicated that miR-134 might be involved in the antidepressant-like effects of Rb1 by promoting the structural plasticity of synapses. Several previous studies have revealed the association of miR-134 with the structural plasticity of synapses. miR-134 was reported to negatively regulate structural plasticity in an animal model of depression [37], and localization of miR-134 to the synapto-dendritic compartment of mammalian hippocampal neurons inhibits dendritic spine development by reducing two important dendritic regulators, LIM-kinase 1 (LIMK1) and Pumilio [38–40].

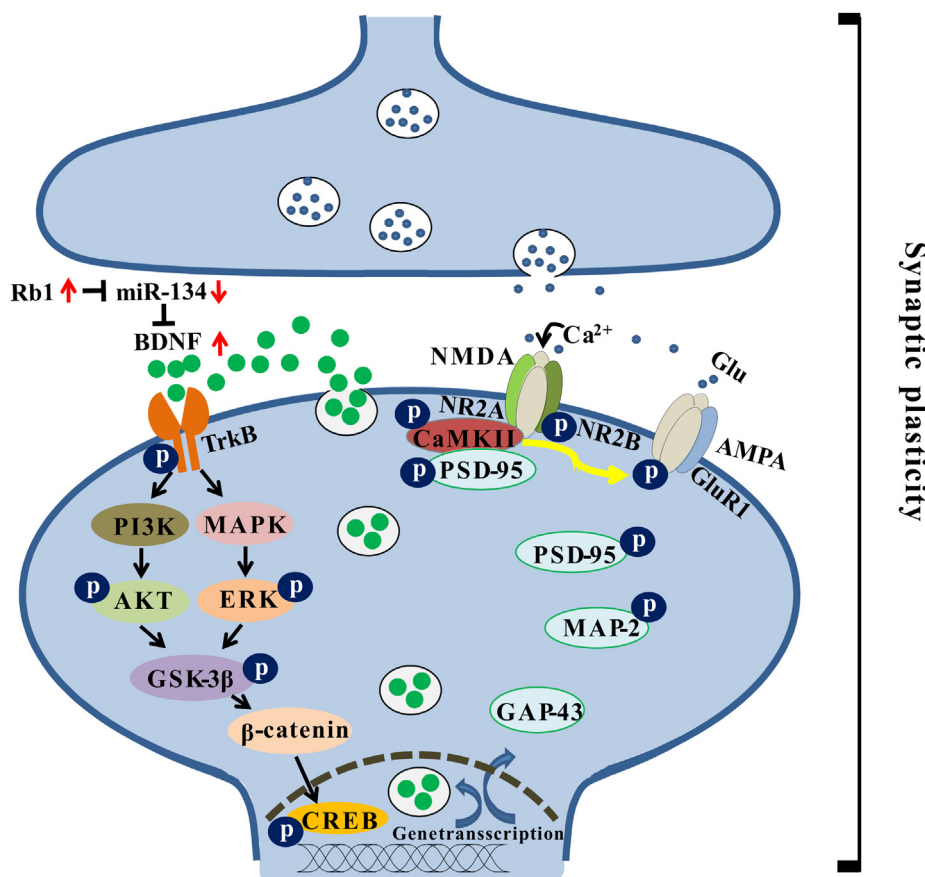


Fig. 6. Schematic diagram of the antidepressant-like effect of Rb1 by potentiating synaptic plasticity via the miR-134-mediated BDNF signaling pathway in a mouse model of chronic stress. Long-term chronic and unpredictable mild stress increase the expression of miR-134 in the mouse hippocampus. The highly expressed miR-134 inhibits the activity of BDNF, thereby inhibiting its receptor TrkB and its downstream PI3K–AKT and MAPK–ERK pathways. Inhibition of both pathways reduces the phosphorylation of the Ser9 site of GSK-3β and then promotes the activation of GSK-3β. Activated GSK-3β reduces the stability of β-catenin, alleviates its binding to CREB in the nucleus, and regulates transcription and expression of genes, such as *BDNF*, *PSD-95*, *GAP-43*, and *MAP-2*. However, Rb1 can inhibit the expression of miR-134 and rescue the negative effects of miR-134 on the BDNF signaling cascade pathway during chronic stress, promoting gene transcription and expression and increasing hippocampal synaptic plasticity. These molecular changes may be the basis for the antidepressant-like effects of Rb1.

Stress negatively induces functional plasticity of synapses and impairs the induction of LTP [41], while facilitating the induction of long-term depression (LTD) in the hippocampus [42]. Synapse-related proteins, including presynaptic GAP-43 and postsynaptic PSD-95 and MAP-2, play crucial roles in the induction and maintenance of LTP [43–45]. Moreover, long-term synaptic potentiation largely depends on the number, location, and activity of receptors in the postsynaptic membrane, especially NMDARs and AMPARs [46]. The influx of Ca^{2+} via NMDAR induces autophosphorylation of CaMKII at Thr286. Activated CaMKII not only binds to the NMDAR NR2B subunit within the PSD region but also catalyzes the phosphorylation of NR2B at Ser1303, increasing the activity of NMDAR. Furthermore, it promotes the activity of the AMPAR GluR1 subunit, increasing the excitatory postsynaptic potential. Notably, the induction of LTP is mainly mediated by postsynaptic membrane NMDARs and then presented by AMPARs [47]. Interestingly, NMDARs in different regions activate different signal transduction pathways and produce contrasting biological effects [48]. Accumulating evidence shows that NMDAR antagonists exert a rapid antidepressant effect, especially ketamine, which was reported to demonstrate a novel role in combating refractory and suicidal depressive disorders by inhibiting the excessive activation of extrasynaptic NR2B [49,50]. In line with these reports, our electrophysiological findings showed that Rb1 induced long-term enhancement of LTP, which was impaired following CUMS exposure. Furthermore, Rb1 demonstrated a significant induction and maintenance effect on LTP by upregulating the expression of PSD-95, GAP-43, MAP-2, NR2A, NR2B, GluR1 and CaMKII in the hippocampus of depression-induced mice. The differences in results of the present study from those obtained for ketamine may be attributed to the high-intensity and long-term external stress stimuli that overactivate extrasynaptic NMDARs, eventually leading to abnormal synaptic function until neuronal cell apoptosis or death. However, these responses to LTP induction and maintenance produced by Rb1 were suppressed by miR-134 overexpression in CUMS-exposed mice.

BDNF-mediated PI3K/AKT and MAPK/ERK intracellular pathways have been implicated in the rapid regulation of synaptic plasticity [10–12]. As a downstream target of PI3K/AKT and MAPK/ERK, GSK-3 β also plays a vital role in regulating synaptic plasticity [51–53]. Increased phosphorylation of GSK-3 β at Ser9 inhibits the activity of GSK-3 β , which in turn causes intracellular β -catenin to enter the nucleus [54], activating the CREB transcription factor to regulate the transcription of various genes, including those encoding BDNF and several other synapse-related proteins [13]. Our data demonstrated that Rb1 significantly increased the expression levels of BDNF and its downstream proteins, including TrkB, AKT, ERK1/2, GSK-3 β , β -catenin and CREB, in CUMS-exposed mice. Herein, we observed that brain-specific miR-134 could directly bind to *BDNF* 3'UTR and was markedly downregulated by Rb1 in the hippocampus of CUMS-exposed mice. Interestingly, the positive effect of Rb1 on the BDNF signaling cascade pathway was inhibited by miR-134 overexpression. These findings indicate that the miR-134-mediated BDNF signaling pathway plays an indispensable role in the antidepressant-like effects of Rb1 and pathogenesis of depression disorders.

In summary, the present study, for the first time, established that miR-134 could bind to *BDNF* and regulate the critical role of BDNF in hippocampal synaptic plasticity. Combined with our previous report assessing Rb1, the antidepressant-like mechanism of Rb1 was further clarified and achieved via the miR-134-mediated BDNF signaling cascade pathway from the perspective of synaptic structural and functional plasticity (Fig. 6). This study provides new evidence for the treatment of stress-related mental disorders with Rb1. In addition to depression-related disorders, the BDNF system is

reportedly involved in neuronal dysfunction diseases, including Alzheimer's disease and Huntington's disease, and Rb1 may play a role in the treatment of these diseases, thus warranting further investigations in the future.

Declaration of competing interest

The authors declare that they have no competing interests.

Acknowledgements

This work was supported by the National Natural Science Foundation of China (81903820), and National Key R&D Program of China (2018YFC2002500).

Appendix A. Supplementary data

Supplementary data to this article can be found online at <https://doi.org/10.1016/j.jgr.2021.03.005>.

References

- [1] Cui W, Ning Y, Hong W, Wang J, Liu Z, Li MD. Crosstalk between inflammation and glutamate system in depression: signaling pathway and molecular biomarkers for ketamine's antidepressant effect. *Mol Neurobiol* 2018;56:3484–500.
- [2] Levy MJF, Fabien B, Steinbusch HW, van den Hove DLA, Kenis G, Lanfumey L. Neurotrophic factors and neuroplasticity pathways in the pathophysiology and treatment of depression. *Psychopharmacology* 2018;235:2195–220.
- [3] Afifi S, Fadel W, Morad H, Eldod A, Gad E, Arfken CL, Samra A, Boutros N. Neuroendocrine study of depression in male epileptic patients. *J Neuropsychiatry Clin Neuro* 2011;23:163–7.
- [4] Marsden WN. Synaptic plasticity in depression: molecular, cellular and functional correlates. *Prog Neuropsychopharmacol Biol Psychiatry* 2013;43:168–84.
- [5] Duman RS, Aghajanian GK, Sanacora G, Krystal JH. Synaptic plasticity and depression: new insights from stress and rapid-acting antidepressants. *Nat Med* 2016;22:238–49.
- [6] Nawa H, Carnahan J, Gall C. BDNF protein measured by a novel enzyme immunoassay in normal brain and after seizure: partial disagreement with mRNA levels. *Eur J Neurosci* 1995;7:1527–35.
- [7] Lu B. BDNF and activity-dependent synaptic modulation. *Learn Mem* 2003;10:86–98.
- [8] Björkholm C, Monteggia LM. BDNF—a key transducer of antidepressant effects. *Neuropharmacology* 2016;102:72–9.
- [9] Madara JC, Levine ES. Presynaptic and postsynaptic NMDA receptors mediate distinct effects of brain-derived neurotrophic factor on synaptic transmission. *J Neurophysiol* 2008;100:3175–84.
- [10] Park H, Poo MM. Neurotrophin regulation of neural circuit development and function. *Nat Rev Neurosci* 2013;14:7–23.
- [11] Luijkart BW, Zhang W, Wayman GA, Kwon CH, Westbrook GL, Parada LF. Neurotrophin-dependent dendritic filopodial motility: a convergence on PI3K signaling. *J Neurosci* 2008;28:7006–12.
- [12] Alonso M, Medina JH, Pozzomiller L. ERK1/2 activation is necessary for BDNF to increase dendritic spine density in hippocampal CA1 pyramidal neurons. *Learn Mem* 2004;11:172–8.
- [13] Bito H, Takemoto-Kimura S. Ca^{2+} /CREB/CBP-dependent gene regulation: a shared mechanism critical in long-term synaptic plasticity and neuronal survival. *Cell Calcium* 2003;34:425–30.
- [14] Tomassoni-Ardori F, Fulgenzi G, Becker J, Barrick C, Palko ME, Kuhn S, Koparde V, Cam M, Yanpallewar S, Oberdoerffer S, et al. RbFox1 up-regulation impairs BDNF-dependent hippocampal LTP by dysregulating TrkB isoform expression levels. *eLife* 2019;8:e49673.
- [15] Levine ES, Dreyfus CF, Black IB, Plummer MR. Brain-derived neurotrophic factor rapidly enhances synaptic transmission in hippocampal neurons via postsynaptic tyrosine kinase receptors. *Proc Natl Acad Sci USA* 1995;92:8074–7.
- [16] Caldeira MV, Melo CV, Pereira DB, Carvalho R, Correia SS, Backos DS, Carvalho AL, Esteban JA, Duarte CB. Brain-derived neurotrophic factor regulates the expression and synaptic delivery of alpha-amino-3-hydroxy-5-methyl-4-isoxazole propionic acid receptor subunits in hippocampal neurons. *J Biol Chem* 2007;282:12619–28.
- [17] Fahimi A, Baktir MA, Moghadam S, Mojabi FS, Sumanth K, McNerney MW, Ponnusamy R, Salehi A. Physical exercise induces structural alterations in the hippocampal astrocytes: exploring the role of BDNF–TrkB signaling. *Brain Struct Funct* 2017;222:1797–808.
- [18] Wang GL, He ZM, Zhu HY, Gao YG, Zhao Y, Yang H, Zhang LX. Involvement of serotonergic, noradrenergic and dopaminergic systems in the antidepressant-

- like effect of ginsenoside Rb1, a major active ingredient of *Panax ginseng* C. A. Meyer. *J Ethnopharmacol* 2017;204:118–24.
- [19] Wang GL, Wang YP, Zheng JY, Zhang LX. Monoaminergic and aminoacidergic receptors are involved in the antidepressant-like effect of ginsenoside Rb1 in mouse hippocampus (CA3) and prefrontal cortex. *Brain Res* 2018;1699:44–53.
- [20] Wang GL, Lei C, Tian Y, Wang YP, Zhang LX, Zhang RH. Rb1, the primary active ingredient in *Panax ginseng* C.A. Meyer, exerts antidepressant-like effects via the BDNF–TrkB–CREB pathway. *Front Pharmacol* 2019;10:1034.
- [21] Shen H, Li Z. miRNAs in NMDA receptor-dependent synaptic plasticity and psychiatric disorders. *Clin Sci* 2016;130:1137–46.
- [22] Ma K, Zhang H, Wei G, Dong Z, Zhao H, Han X, Song X, Zhang H, Zong X, Baloch Z, et al. Identification of key genes, pathways, and miRNA/mRNA regulatory networks of CUMS-induced depression in nucleus accumbens by integrated bioinformatics analysis. *Neuropsychiatr Dis Treat* 2019;15:685–700.
- [23] Willner P, Towell A, Sampson D, Sophokleous S, Muscat R. Reduction of sucrose preference by chronic unpredictable mild stress, and its restoration by a tricyclic antidepressant. *Psychopharmacol* 1987;93:358–64.
- [24] Egawa J, Zemljic-Harpf A, Mandyam CD, Niesman IR, Lysenko LV, Kleschevnikov AM, Roth DM, Patel HH, Patel PM, Head BP. Neuron-targeted caveolin-1 promotes ultrastructural and functional hippocampal synaptic plasticity. *Cereb Cortex* 2018;28:3255–66.
- [25] Porsalt RD, Bertin A, Jalife M. Behavioral despair in mice: a primary screening test for antidepressants. *Arch Int Pharmacodyn* 1977;229:327–36.
- [26] Li XL, Yuan YG, Xu H, Wu D, Gong WG, Geng LY, Wu FF, Tang H, Xu L, Zhang ZJ. Changed synaptic plasticity in neural circuits of depressive-like and escitalopram-treated rats. *Int J Neuropsychopharmacol* 2015;18:1–12.
- [27] Egawa J, Zemljic-Harpf A, Mandyam CD, Niesman IR, Lysenko LV, Kleschevnikov AM, Roth DM, Patel HH, Patel PM, Head BP. Neuron-targeted caveolin-1 promotes ultrastructural and functional hippocampal synaptic plasticity. *Cereb Cortex* 2018;28:3255–66.
- [28] Varendi K, Kumar A, Härma MA, Andressoo JO. miR-1, miR-10b, miR-155, and miR-191 are novel regulators of BDNF. *Cell Mol Life Sci* 2014;71:4443–56.
- [29] Varendi K, Märtilik K, Andressoo JO. From microRNA target validation to therapy: lessons learned from studies on BDNF. *Cell Mol Life Sci* 2015;72:1779–94.
- [30] Wang Z, Yang P, Qi Y. Role of microRNA-134 in the neuroprotective effects of propofol against oxygen-glucose deprivation and related mechanisms. *Int J Clin Exp Med* 2015;8:20617.
- [31] Cattaneo A, Cattane N, Begni V, Pariante CM, Riva MA. The human BDNF gene: peripheral gene expression and protein levels as biomarkers for psychiatric disorders. *Transl Psychiatry* 2016;6:e958.
- [32] Darcq E, Warnault V, Phamluong K, Besserer GM, Liu F, Ron D. MicroRNA-30a-5p in the prefrontal cortex controls the transition from moderate to excessive alcohol consumption. *Mol Psychiatry* 2014;20:1219–31.
- [33] Kang HJ, Voleti B, Hajszan T, Rajkowska G, Stockmeier CA, Licznarski P, Lepack A, Majik MS, Jeong LS, Banasr M, et al. Decreased expression of synapse-related genes and loss of synapses in major depressive disorder. *Nat Med* 2012;18:1413–7.
- [34] Chai H, Liu B, Zhan H, Li X, He Z, Ye J, Guo Q, Chen J, Zhang J, Li S. Antidepressant effects of rhodomyltone in mice with chronic unpredictable mild stress-induced depression. *Int J Neuropsychopharmacol* 2018;22:157–64.
- [35] Yau SY, Li A, Zhang ED, Christie BR, Xu A, Lee TM, So KF. Sustained running in rats administered corticosterone prevents the development of depressive behaviors and enhances hippocampal neurogenesis and synaptic plasticity without increasing neurotrophic factor levels. *Cell Transplant* 2014;23:481–92.
- [36] Yong Z, Yan L, Gao X, Gong Z, Su R. Effects of thienorphine on synaptic structure and synaptophysin expression in the rat nucleus accumbens. *Neuroscience* 2014;274:53–8.
- [37] Fan CQ, Zhu XZ, Song QQ, Wang P, Liu Z, Yu SY. MiR-134 modulates chronic stress-induced structural plasticity and depression-like behaviors via downregulation of Limk1/cofilin signaling in rats. *Neuropharmacology* 2018;131:364–76.
- [38] Gao J, Wang WY, Mao YW, Gräff J, Guan JS, Pan L, Mak G, Kim D, Su SC, Tsai LH. A novel pathway regulates memory and plasticity via SIRT1 and miR-134. *Nature* 2010;466:1105–9.
- [39] Schrott GM, Tuebing F, Nigh EA, Kane CG, Sabatini ME, Kiebler M, Greenberg ME. A brain-specific microRNA regulates dendritic spine development. *Nature* 2006;439:283–9.
- [40] Morinobu S. Physiopathological mechanism of depression in relation to neurotrophic and growth factors and synaptic plasticity. *Psychiatria et neurologia Japonica* 2009;111:687–91.
- [41] Keralapurath MM, Clark JK, Hammond S, Wagner JJ. Cocaine- or stress-induced metaplasticity of LTP in the dorsal and ventral hippocampus. *Hippocampus* 2014;24:577–90.
- [42] Cao J, Chen N, Xu TL, Xu L. Stress-facilitated LTD induces output plasticity through a synchronized-spikes and spontaneous unitary discharges the CA1 region of the hippocampus. *Neurosci Res* 2004;49:229–39.
- [43] Luo Y, Vallano ML. Arachidonic acid, but not sodium nitroprusside, stimulates presynaptic protein kinase C and phosphorylation of GAP-43 in rat hippocampal slices and synaptosomes. *J Neurochem* 2010;64:1808–18.
- [44] Dmitry T. The distribution of synaptic strengths and possible mechanism for synaptic plasticity arise in the model of inter-spine molecular transport of PSD-95 molecules. *J Neurophysiol* 1999;82:1097–113.
- [45] Soderling TR. Modulation of glutamate receptors by calcium/calmodulin-dependent protein kinase II. *Neurochem Int* 1996;28:359–61.
- [46] Jang SS, Royston SE, Xu J, Cavaretta JP, Vest MO, Lee KY, Lee S, Jeong HG, Lombroso PJ, Chung HJ. Regulation of STEP61 and tyrosine-phosphorylation of NMDA and AMPA receptors during homeostatic synaptic plasticity. *Mol Brain* 2015;8:55.
- [47] Zhu YB, Jia GL, Wang JW, Ye XY, Lu JH, Chen JL, Zhang MB, Xie CS, Shen YJ, Tao YX, et al. Activation of CaMKII and GluR1 by the PSD-95-GluN2B coupling-dependent phosphorylation of GluN2B in the spinal cord in a rat model of type-2 diabetic neuropathic pain. *J Neuropathol Exp Neurol* 2020;79:800–8.
- [48] Zhou XJ, Chen ZY, Yun WW, Ren J, Li C, Wang H. Extrasynaptic NMDA receptor in excitotoxicity: function revisited. *Neuroscientist* 2014;21:337–44.
- [49] Rachael I, Heather K, Stafford L, Jane DE, Bortolotto ZA, Collingridge GL, Lodge D, Volianskis A. Some distorted thoughts about ketamine as a psychodelic and a novel hypothesis based on NMDA receptor-mediated synaptic plasticity. *Neuropharmacol* 2018;142:30–40.
- [50] Li SX, Han Y, Xu LZ, Yuan K, Zhang RX, Sun MO, Lee KY, Xu DF, Yuan M, Deng JH, Meng SQ, et al. Uncoupling DAPK1 from NMDA receptor GluN2B subunit exerts rapid antidepressant-like effects. *Mol Psychiatry* 2018;23:597–608.
- [51] Aceto G, Colussi C, Leone L, Fusco S, Rinaudo M, Scala F, Green TA, Laezza F, D'Ascenzo M, Grassi C. Chronic mild stress alters synaptic plasticity in the nucleus accumbens through GSK3β-dependent modulation of Kv4.2 channels. *Proc Natl Acad Sci USA* 2020;117:1–11.
- [52] Chiu CH, Chyau CC, Chen CC, Lee LY, Chen WP, Liu JL, Lin WH, Mong MC. Erinacine a-enriched hericium erinaceus mycelium produces antidepressant-like effects through modulating BDNF/PI3K/Akt/GSK-3β signaling in mice. *Int J Mol Sci* 2018;19:341.
- [53] Filippo C, Elisa G, Marco C, Failla M, Rosa CL, Crimi N, Sortino MA, Nicoletti F, Copani A, Vancheri C. TGF-β1 targets the GSK-3β/β-catenin pathway via ERK activation in the transition of human lung fibroblasts into myofibroblasts. *Pharmacol Res* 2008;57:274–82.
- [54] Garza JC, Guo M, Zhang W, Lu XY. Leptin restores adult hippocampal neurogenesis in a chronic unpredictable stress model of depression and reverses glucocorticoid-induced inhibition of GSK-3β/β-catenin signaling. *Mol Psychiatry* 2012;17:790–808.